Scientific Research and Essays Vol. 5(18), pp. 2694-2701, 18 September, 2010
Available online at http://www.academicjournals.org/SRE
ISSN 1992-2248 ©2010 Academic Journals

Full Length Research Paper

Numerical simulation of dynamic side impact test for an aluminium alloy wheel

Muhammet Cerit

Department of Mechanical Engineering, Sakarya University, Esentepe 54187, Sakarya, Turkey.
E-mail: mcerit@sakarya.edu.tr. Tel: +90 264 295 58 54. Fax: +90 264 295 56 01.

Accepted 23 August, 2010

A great number of wheel test are requited in designing and manufacturing of wheels to meet the safety requirements. The impact performance of wheel is a major concern of a new design. The test procedure has to comply with international standards, which establishes minimum mechanical requirements, evaluates axial curb and impact collision characteristics of wheels. Numerical implementation of impact test is essential to shorten the design time, enhance the mechanical performance and lower development cost. This study deals with the simulation of impact test for a cast aluminium alloy wheel by using 3–D explicit finite element methods. A numerical model of the wheel with its tire and striker were developed taking account of the nonlinearity material properties, large deformation and contact. Simulation was conducted to investigate the stress and displacement distributions during wheel impact test. The analyses results are presented as a function of time. The maximum value of the displacement and stress on the wheel and tire are shown. As a result, the use of explicit finite element method to predict the performance of new products design is replacing the use of physical test.

Key words: Light alloy wheel, impact test, explicit finite element analyses, computational mechanics.

INTRODUCTION

Road wheel is an important structural member of the vehicular suspension system that supports the static and dynamic loads encountered during vehicle operation. Since the rims, on which cars move, are the most vital elements in a vehicle, they must be designed carefully. Safety and economy are particularly of major concerns when designing a mechanical structure so that the people could use them safely and economically. Style, weight, manufacturability and performance are the four major technical issues related to the design of a new wheel and/or its optimization (Carvalho et al., 2001; Kouichi et al., 2002). The wheels are made of either steel or cast/forge aluminium alloys. Aluminium is the metal with features of excellent lightness, corrosion resistance, etc. In particular, the rims, which are made of aluminium casting alloys, are more preferable because of their weight and cost.

Automotive manufacturers have been developing safe, fuel efficient and lightweight vehicular components to meet governmental regulations and industry standards (Stearns, 2000). In the real service conditions, the determination of mechanical behaviour of the wheel is important, but the testing and inspection of the wheels during their development process is time consuming and costly. For economic reasons, it is important to reduce the time spent during the development and testing phase of a new wheel. A 3–D stress analysis of aluminium car road wheels involves complicated geometry. Therefore, it is difficult to estimate the stresses by using elementary mechanical approximations. For this purpose, Finite Element Analysis (FEA) is generally used in the design stage of product development to investigate the mechanical performance of prototype designs (Shang et al., 2004). FEA simulation of the wheel tests can significantly reduce the time and cost required to finalise the wheel design. Thus, the design modifications could be conducted on a component to examine how the change would influence its performance, without making costly alteration to tooling and equipment in real production. Therefore, in order to replace the physical test, the FEA simulation of the impact test should supply reliable results and sufficient information. In this regard, it is important to evaluate the effect of the tire portion on the wheel impact performance during the wheel impact

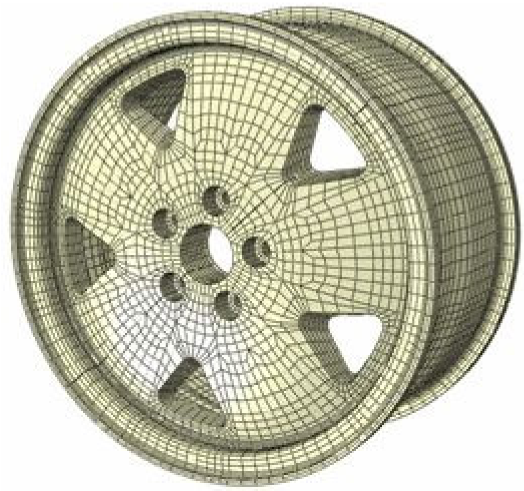

Figure 1. The Finite Element Model of aluminium alloy wheel.

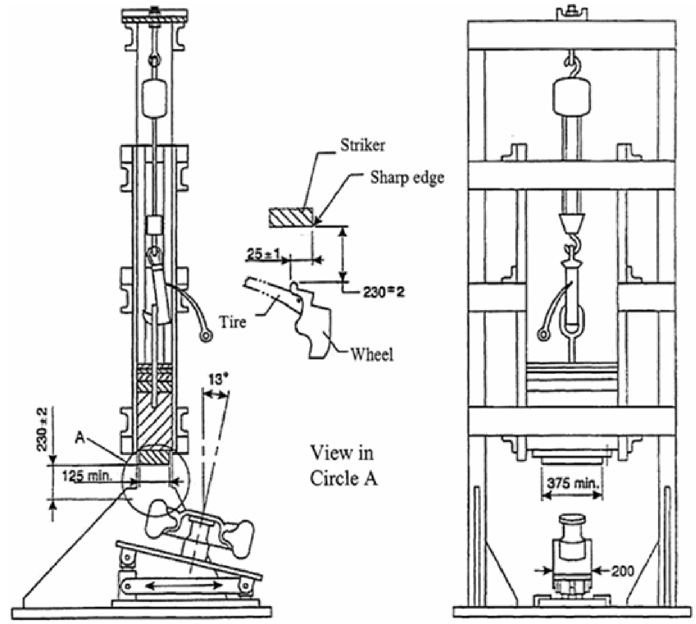

Figure 2. Schematic diagram of wheel impact test machine.

test.

In this study, finite element analysis was conducted to simulate a cast aluminium wheel, shown in Figure 1, for the impact test according to the standard ISO 7141, using commercial ABAQUS/ explicit code. The numerical model of an aluminium alloy wheel with its tire and striker were generated taking into account, the large deformable, highly non–linear material properties and contact nonlinearity. In the case of strike that changes its magnitude and direction within a very short time, explicit coded software that considers dynamic forces as well as static forces is employed rather than implicit method used for static problems. The model includes elasto–plastic and hyper elastic material for aluminium and rubber, respectively. The tire (made of vulcanized rubber and a reinforcing carcass) is a highly anisotropic, viscoelastic and composite structure. To obtain realistic response from tire models, essential features must be included into the tire model.

IMPACT TEST EQUIPMENT AND PROCEDURE

Mechanical performance of road wheels under normal or severe driving conditions is evaluated by using three standard methods, such as dynamic impact, radial fatigue and rotary fatigue tests. The rotating bending test simulates cornering induced loads by applying a constant rotating bending moment to the wheel. In the radial fatigue test, the wheel and tire assembly are loaded radially against a constantly rotating drum to simulate the radial loading on the wheel. The wheel impact test is used to evaluate the impact performance, in which the striker is dropped from a specified height above the tire–wheel assembly. It is considered to be the case where the wheel collides with the curb of the road or a large obstacle. The test is designed to evaluate the frontal impact resistance of wheel and tire assemblies used in all cars and multi–purpose vehicles. The test is specifically related to vehicle pothole tests that are undertaken by most vehicle manufacturers. The scope has been expanded to allow the use of a striker that can be angled to preferentially impact the inboard and outboard wheel flange. Before the test, a wheel undergoes complete visual inspection to ensure that no cracks exist in the body. In order to pass the impact test, the wheel must meet the following minimum performance standards: There will no visible fracture of the central member of the wheel assembly, no separation of the central member from the rim, no sudden loss of tire air pressure and deformation of the wheel assembly, or fracture in the area of the rim section contracted by the faceplate weight system do not constitute a failure (International standard, 1995).

The impact test standard provides detailed test procedures and equipment description for the impact test. A test machine is shown schematically in Figure 2. The test set up, in which a striker applies an impact to the rim flange of a wheel, included a tire. The wheels are mounted with its axis at an angle of 13 degrees (± 1 degree) to the vertical, so that its highest point is presented to the vertically acting striker. The impacting face of the striker is at least 125 mm wide and 375 mm long. The freely dropping height of the striker is 230 mm (± 2 mm) above the highest point of the rim flange. The striker is placed over the tire and its edge overlaps the rim flange by 25 mm. The inflation pressure of the tire can be specified by manufacturer taking into account, the serves conditions. An inflation pressure of 200 kPa, which in real service condition, was applied on the inner

Table 1. Mechanical properties of aluminium alloy wheel.

Elasticity modulus	Poisson's ratio	Yield stress	Ultimate stress	Fracture strain
64 GPa	0.34	218 MPa	283 MPa	0.072

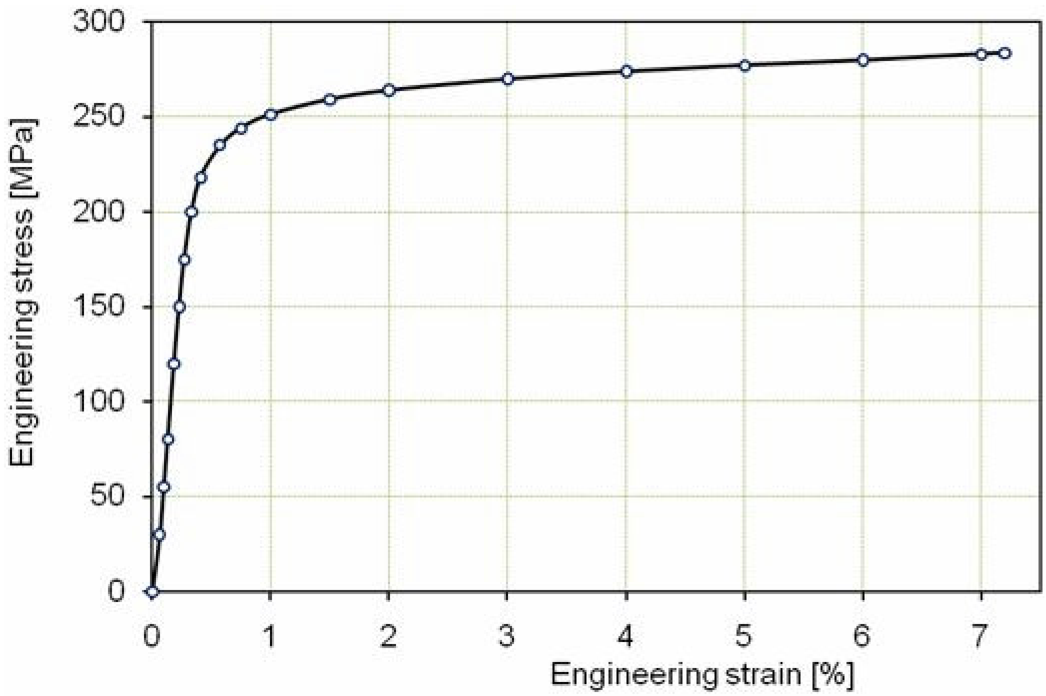

Figure 3. Engineering stress–strain of aluminium alloy.

surface of tire and portion rim (International Standard, 1995).

MATERIAL PROPERTIES

The material properties of A356 cast aluminium alloy that is widely used in automotive engineering industry was considered in the FE simulation. Mechanical properties of aluminium alloy are given in Table 1.

A nonlinear elasto–plastic material model was used to describe the material behaviour of aluminium wheel in the dynamic analyses. The engineering stress–strain curve of the aluminium alloy is plotted in Figure 3 (Shang and Altenhof, 2005). True stress–strain material data are required for input into the finite element model. The engineering stress–strain curve data were converted into the true stress–strain curve data and then imported into the FEA model. Equations (1) and (2) were used to calculate the true stress–strain values of the aluminium alloy:

$$\varepsilon_{true} = \ln\left(1 + \varepsilon_{eng}\right) \quad (1)$$

$$\sigma_{true} = \sigma_{eng}\left(1 + \varepsilon_{eng}\right) = \frac{F}{A_0}\left(1 + \varepsilon_{eng}\right) \quad (2)$$

A typical pneumatic radial tire consists of a specific combination of rubber compounds, cord and steel belts. The main parts of a modern pneumatic tire are its body, sidewalls, beads, and tread as shown in Figure 4. The body is made of layers of rubberized fabric, called plies, that gives the tire strength and flexibility. The fabric is made of rayon, nylon, or polyester cord. Covering the plies are sidewalls and tread of chemically treated rubber. The sidewalls form the outer walls of the tire. Embedded in the two inner edges of the tire are steel loops, called bead, that hold the tire to the wheel. The rubber components have different characteristics independence of their functionality (Tönük and Ünlüsoy, 2001). The main body of the tire is hyper elastic rubber that shows a nonlinear stress–strain relationship. Average tire material characteristic can be described by the Mooney–Rivlin material formulation, which is nearly identical to two constants parameter. This behaviour is well described by the Mooney–Rivlin material formulation included in the ABAQUS software. Mooney–Rivlin constants C01 and C10 are given Table 2 (Tönük and Ünlüsoy, 2001). Steel reinforcement is modelled by linear elastic material.

The striker used in the dynamic analysis was modelled as an elastic material using steel material properties. Young's modulus is 200 GPa, Poisson's ratio is 0.3 and density is 7850 kg/m^3.

EXPLICIT FINITE ELEMENT ANALYSIS

Modelling the mechanical response of impact test rim is extremely complex and involves taking into account both non–linear analyses for the tire and rim portion. The interface of the two components

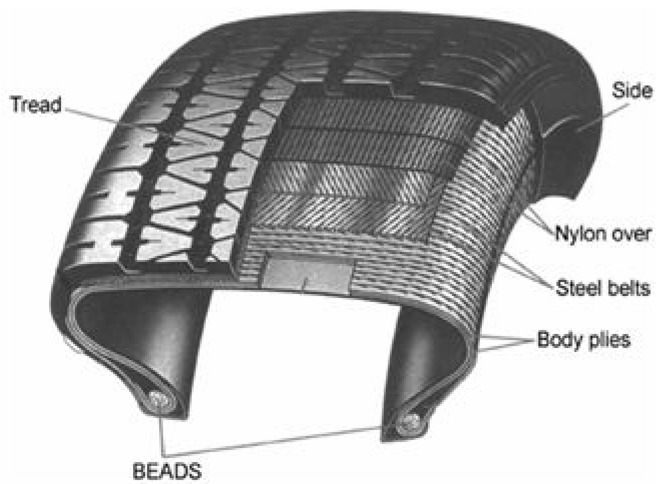

Figure 4. A typical pneumatic tire combination.

Table 2. Mooney–Rivlin constants of tire's materials components.

Materials	Bead filler	Sidewall	Under tread	Tread
C01 [MPa]	21.26	0.8303	0.427	1.805
C10 [MPa]	14.14	0.1718	0.1404	0.806

can be established using general contact elements. Commercial finite element ABAQUS/explicit code is utilized to perform 3–D dynamic analysis of wheel impact test. It has large deformable capability, contact nonlinearity and highly non–linear material models. The numerical modelling of wheel impact test obeys the experimental procedure, which was described in the ISO 7141. The modelled wheel is 487.4 mm (19 in) diameter with 203.2 mm (8 in) width. The whole of numerical model is an assembly consisting of three portions, namely a wheel, tire and striker shown in Figure 5.

Uniform shapes and forms of elements play important role in the sensitivity of the results when using the explicit finite element method. Therefore, the meshing of the wheel, tire and impact striker models is mainly constructed by 3–D structural solid having 20–node finite element. It can tolerate irregular shapes without much loss of accuracy. The tire model was generated based on the tire geometry. However, including every detail, it makes the model too complicated to be solved within a reasonable time limit. In order to simplify and reduce the overall size of the model, some of the features which are not essential in cornering, are either simplified.

The wheel has symmetry with respect to the geometry, loading and boundary condition, half part is modelled in order to reduce CPU time. Symmetric constraints are imposed on the symmetric plane of the model. All degrees of freedom of the nodes on the mounting surface of the hub and bolt holes were fully constrained. To avoid slipping, the contact boundary condition was modelled among the striker, wheel and tire. Friction coefficient was assumed to be 0.3 of that surface. The nodes at the surface between the wheel and striker are constrained to move together. The halved model including rim, tire and striker compose of 26313 elements.

The mass of the striker is a variable related to the maximum static wheel load as presented in Equation 3. The unit of mass is kilogram:

$$m = 0.6 \times m_w + 180 \qquad (3)$$

where m is the mass of striker, and m_w is the maximum static wheel loading as specified by the wheel and/or vehicle manufacturer. Mass of the striker for the half part of the wheel–tire was determined to be 468 kg. The volume of the striker was adjusted so that the total mass of the striker is the same as that of the striker used in a real impact test. Striker dimensions are 627 mm in height, 250 mm in width and 380 mm in length.

The striker was constrained in the horizontal direction to ensure that the striker could only be displaced vertically as in the impact test. For the purpose of reducing computational time, the initial dropping height, which represents the distance between the lower surface of the striker and the impact point on the rim flange, was modified from the prescribed value of 230 mm to 0, but with similar impact energy. The magnitude of the initial velocity of the striker prior to impact was calculated using the following equation and applying the energy conservation principle (Meriam and Kraige, 2003).

$$V = \sqrt{2gh} \qquad (4)$$

where V is the initial impact velocity of the striker, g is the acceleration of gravity and $h = 0.23\ m$ is the initial height of the striker.

It is important to determine time step in the explicit FE analysis. For nonlinear analysis, time step size may become small because of convergence difficulties. The maximum time step for stable dynamic response based on the explicit integration method can be determined by the following criteria:

$$\Delta t \leq [(\Delta t)]_{cr} \leq l_e / C = l_e / \sqrt{E/\rho} \qquad (5)$$

where l_e is the smallest size of the element for the analysis model. Parameter C is the wave propagation velocity, E is Young's modulus, and ρ is the density (ABAQUS/Explicit user's manual, 2006; Analysis User's Manual, 2006).

The automatic incremental time step in software is used to calculate the dynamical response that the time step during calculation varied with the nonlinear effects of the structure. In the analysis, average element size is 7 mm and minimum edge length is 1.2 mm. The minimum time step for automatic time step during the response is 4.5×10^{-8} s. Total time and sub step size are selected as 50 and 100 ms, respectively. Results are recorded at every 0.5 ms.

Owing to ductile characteristic of aluminium, von Mises yield criterion can also be formulated in terms of the von Mises or equivalent stress (Chang, 2008). The material yields at the critical point when von Mises stress reaches the yield point. The equivalent stress is considered to determine whether the material yields or not (Hibbeler, 2003). Expressing the von Mises stress in terms of the principal stress components can be determined using Equation 6.

$$\sigma_{eq} = \sqrt{\frac{(\sigma_1 - \sigma_2)^2 + (\sigma_1 - \sigma_3)^2 + (\sigma_2 - \sigma_3)^2}{2}} \qquad (6)$$

NUMERICAL RESULTS AND DISCUSSION

Due to the extreme short duration of wheel impact test, it is not easy to ascertain the wheel impact response during contact, based on evaluation of the experimental specimens after the test. However, numerical simulation

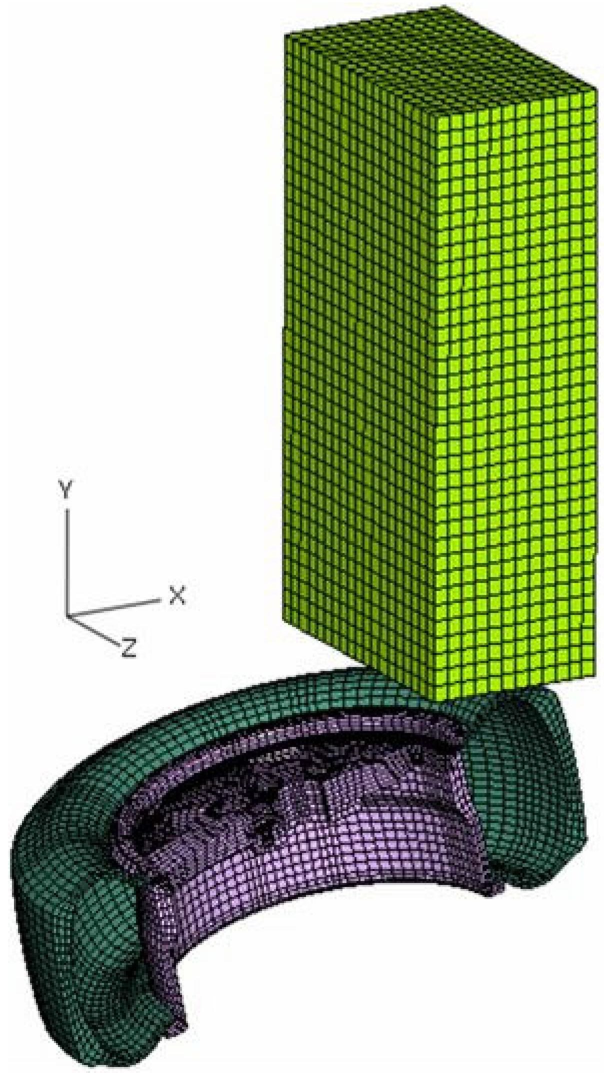

Figure 5. Finite element model of the wheel–tire assembly and striker.

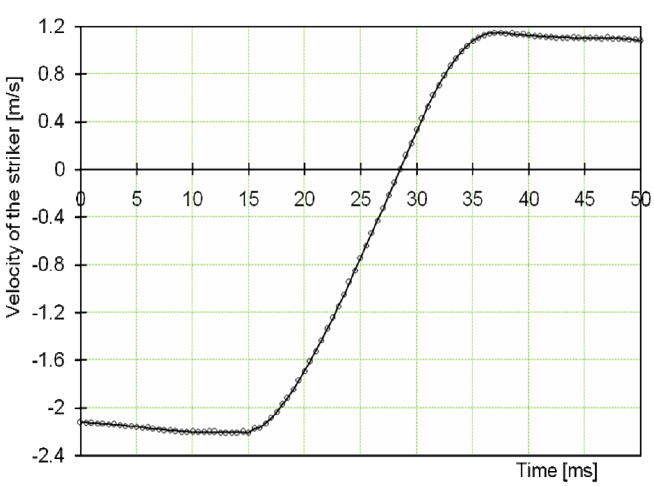

Figure 6. Variation of the striker velocity with time during impact.

may be capable of providing direct observations during the entire impact test. Explicit finite element analysis carried out for 50 ms and the results were recorded at 0.5 ms time interval.

For the FE model with the tire portion, the striker makes instant contact with the tire at a velocity of 2.12 m/s. During the time 0 -15 ms, the striker has impacted on the tire with a slight increase of its downward velocity. After 15 ms, the striker velocity decreases quickly with a constant drop rate of 0.15 m/ms and reach zero at 28.5 ms. From 15 - 28.5 ms, the kinetic energy of the striker decreased to zero due to the work of the contact force generating both elastic and plastic deformation within the wheel. After 28.5 ms, the striker regains an upward velocity, which is a result of the elastic deformation recovery for the wheel and tire. The upward velocity of the striker increases to its highest point of approximately 1.1 m/s and then decreases as a result of gravity acting on the reverse direction of motion. Figure 6 illustrates the velocity of the striker as a function of time for the FE model of the wheel–tire assembly. The maximum deformation, based on the numerical simulation results obtained by applying the FE model with the tire portion, is illustrated in Figure 7. The majority of deformations observed during the impact were found to be almost 50.21 mm for the tire portion. The maximum displacement of the wheel occurred at the flange and its magnitude is 16.3 mm. This is primarily due to the fact that the tire is essentially hyper elastic materials, whereas, the wheel is a metal nature. Figure 8 shows that the variations of the displacement for both striker and flange edge with time during impact. Due to the plastic deformation arising as a result of impact, the wheel shape will change significantly. The plastic deformation response is typically expressed by the bottom flange shape variation from the original circle to an elliptic shape. Equivalent stress contour distributions in the wheel tire assembly are shown in Figure 9. The stress level is relatively low from 0 - 15 ms. When the striker contact with flange edge, a sharp increase is observed in equivalent stress and its magnitude reaches 192 MPa at 15 ms. The deformation of aluminium alloy before the yield point, generates only elastic strains, which are fully recovered if the applied load is removed. However, once the effective von Mises stress in the metal exceeds the material yield strength, permanent deformation sets in. The results from uniaxial tension tests were used to compare simulation with the predicted stresses according to the von Mises yield criterion. von Mises stress attains the yielding point of aluminium alloy at about 16.5 ms. When von Mises stress is higher than 218 MPa (exceeding yield strength), the material start yielding. After that time, von Mises stress increases slowly, while deformations proceed from 16.5 -28.5 ms. It can be explained that plastic deformation has taking place.

Figure 10 indicates that for the first 15 ms, there is slightly an oscillation near 10 MPa, which is relatively very low. However, there is a sharp increase in the von

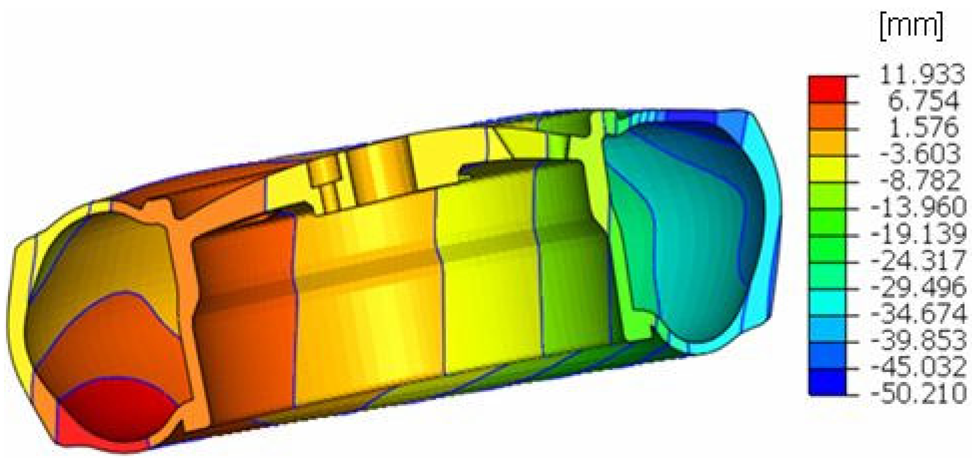

Figure 7. Displacement on wheel–tire assembly at the zero velocity of the striker.

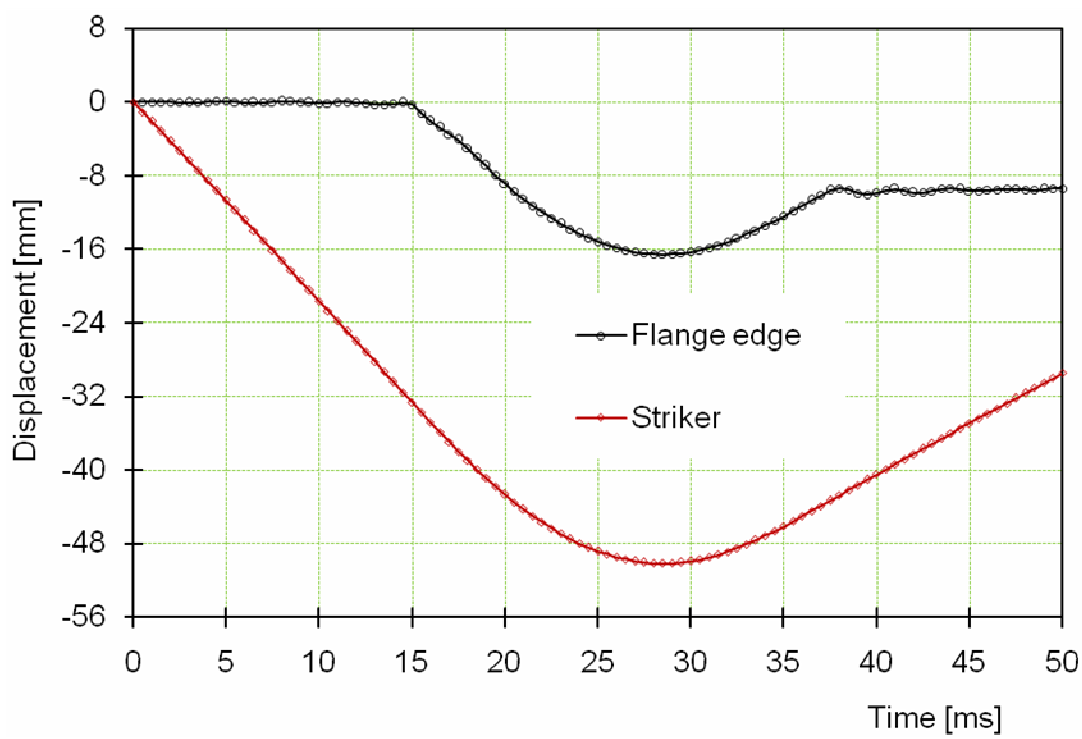

Figure 8. Variations of both striker and flange edge displacement with time.

Mises stress due to the contact it has with the wheel and it behaves almost in a linear manner because of a yield in the wheel. This continues until the striker comes to full stop, then it reversibly begins to increase at the same rate up to maximum stress. The oscillation of the stress after 36th ms is dampened by motion of both tire and wheel. Although severe plastic deformation takes place or equivalent stress exceeding yield strength, wheel is not fractured.

Figure 11 illustrates the maximum von Mises stress contours for wheel–tire assembly when the striker comes to full stop during the impact. It is clear that the maximum equivalent stress is seen around the lug region, so a permanent plastic deformation is observed in this region as expected. Maximum stress is seen as if it occurs in the contact region. Therefore, the maximum equivalent stress takes place in the lug region as expected, since the moment generated by the striker is highest with respect to an axis passing through lug region. Furthermore, due to lug holes, geometrical complexity would contribute

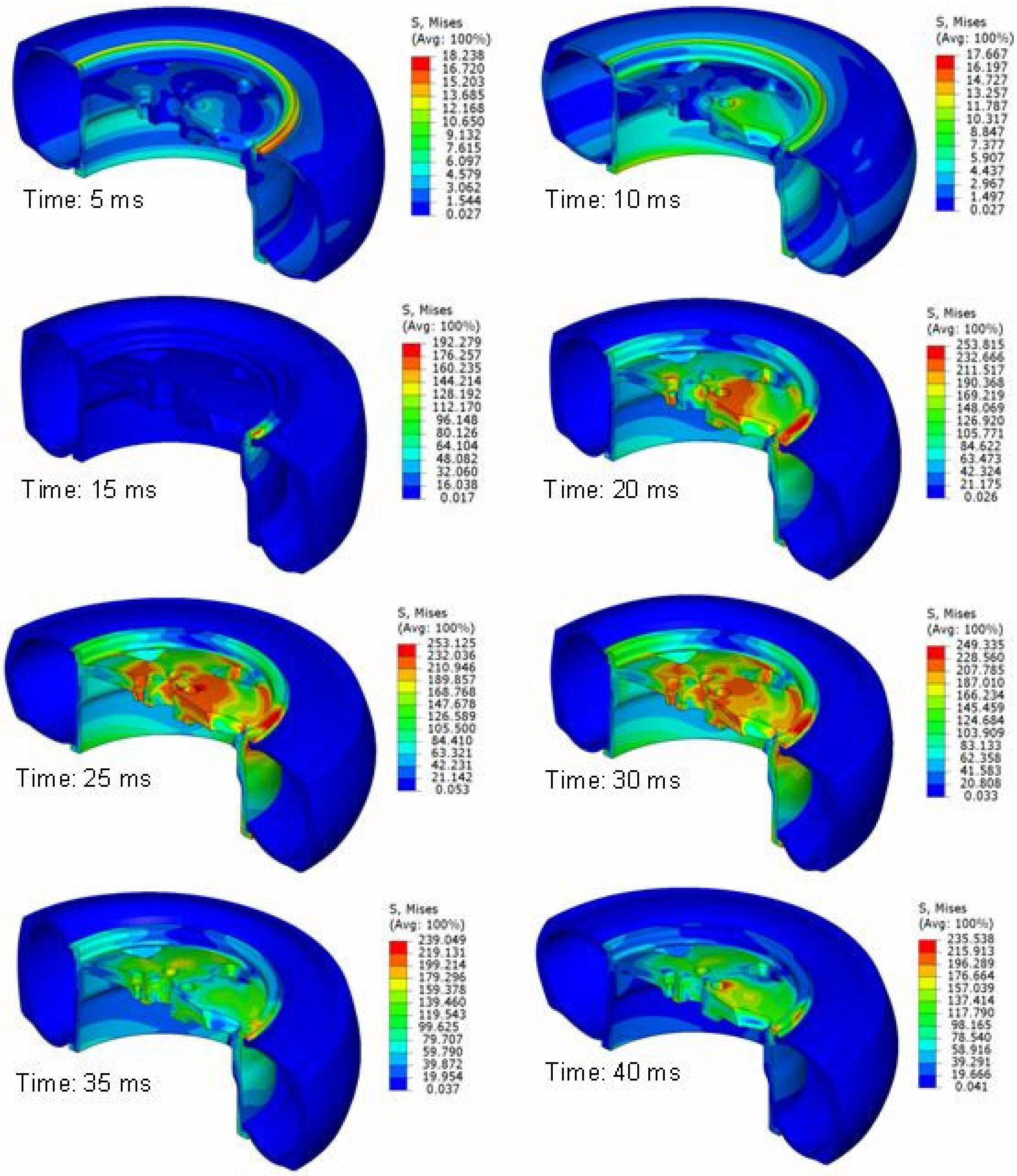

Figure 9. Variation of von Mises stress contour with time on the wheel–tire assembly.

additional stress intensity in this region.

Conclusion

The dynamic response of a wheel–tire assembly during the impact test is a highly nonlinear phenomenon. In this paper, a numerical study of impact test of the wheel–tire assembly was performed using explicit finite element code. 3–D finite element analysis with a reasonable mesh size and time step can reliably estimate the dynamic response. Such results will help to predict the locations, in which the failure may take place during impact test and improve the design of a wheel with required mechanical performance. The result showed that the maximum stress takes place in the lug region of the wheel. This is primarily due to the fact that the lug hole forms geometrical complexities and irregularities in this region. Moreover, the moment generated by the striker is highest with respect to an axis passing through lug region. As a result, non linear simulation can be very useful in the optimisation phase in the design of the wheel.

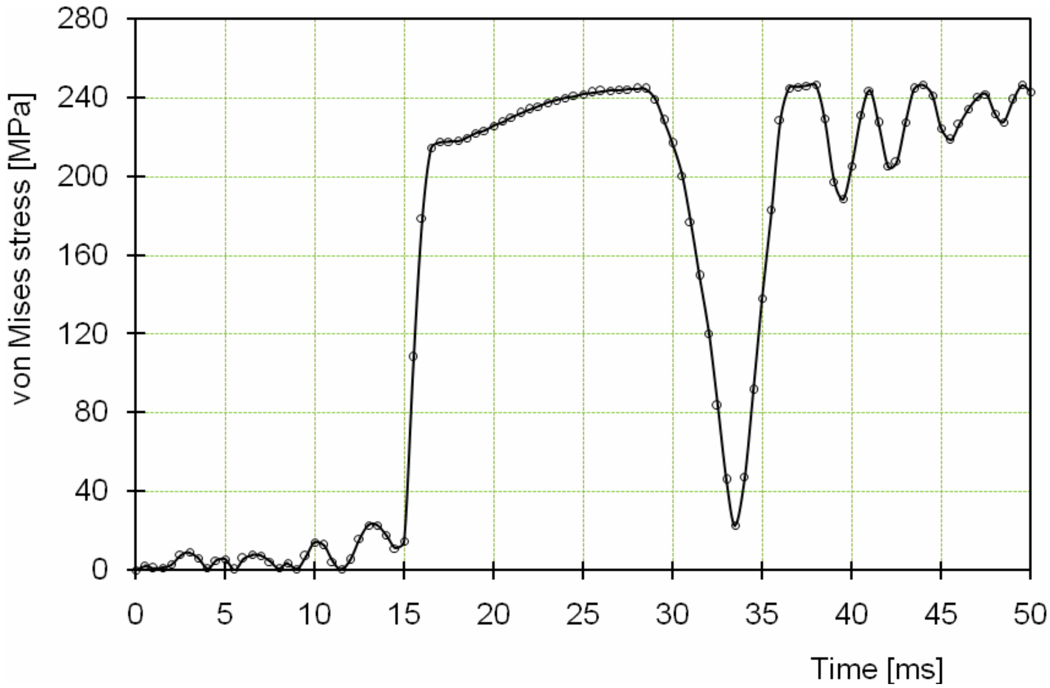

Figure 10. Variation of von Mises stress with time in the lug region during impact.

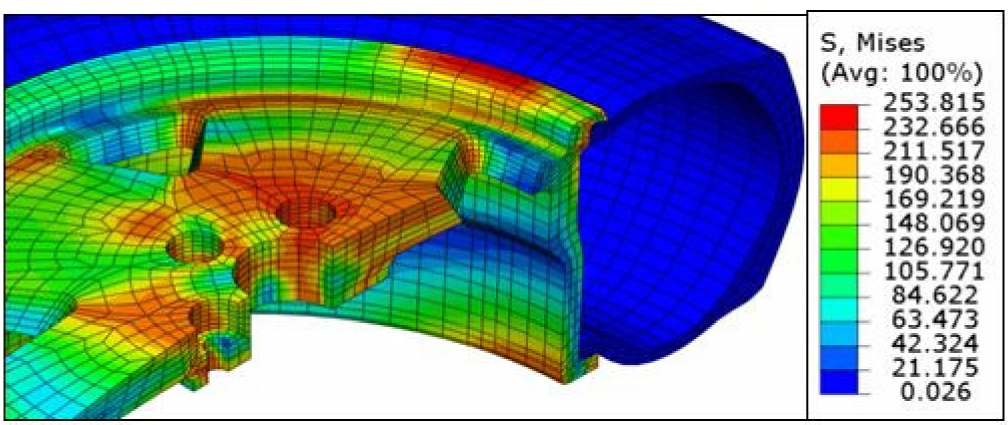

Figure 11. von Mises stress contour on the wheel tire with zero velocity of the striker.

REFERENCES

ABAQUS/Explicit user's manual V 6.6, (2006).

Analysis User's Manual V 6.6, (2006).

Chang C (2008). Modelling for impact test of aluminum wheels, Ph. D. Thesis, Department of Mechanical Engineering, National Central University, Taiwan.

Carvalho C, Voorwald H, Lopes C (2001). Automotive Wheels – An Approach for Structural Analysis and Fatigue Life Prediction, SAE paper no. 2001–01–4053, SAE 2001 World Congress, Detroit.

Hibbeler RC (2003). Mechanics of materials, Pearson Education Inc.

International Standard (1995). ISO 7140 include passengers cars light alloy wheels impact test.

Kouichi A, Ryoji I (2002). Shortening Design and Trial Term for Aluminum Road Wheel by CAE, Casting Technology (Japanese), 74: 533-538.

Meriam JL, Kraige LG (2003). Engineering mechanics, Dynamics, 5. Edition, Jonh Wiley and Sons.

Shang R, Li N, Altenhof W, Hu H (2004). Dynamic side impact simulation of aluminum wheels incorporating material property variations, Aluminum (The Minerals, Metals & Materials Society).

Shang R, Altenhof W (2005). Wheel impact performance with consideration of material in homogeneity and a simplified approach for modeling, Int. J. Crashworthiness, 10: 137-150.

Stearns JC (2000). An investigation of stress and displacement distribution in a aluminum alloy automobile rim, Ph.D. Thesis, The Graduate Faculty of the University of Akron.

Tönük E, Ünlüsoy YS (2001). Prediction of automobile tire cornering force characteristics by finite element modeling and analysis, Comput. Struct., 79(13): 1219-1232.